Available online at www.sciencedirect.com
ScienceDirect
Journal of Power Sources 167 (2007) 504–509
JOURNAL OF POWER SOURCES
www.elsevier.com/locate/jpowsour

Short communication

Performance improvement of $LiCoO_2$ by molten salt surface modification

Ying Bai, Hongjun Shi, Zhaoxiang Wang *, Liquan Chen

Laboratory for Solid State Ionics, Institute of Physics, Chinese Academy of Sciences, Beijing 100080, China

Received 5 December 2006; received in revised form 12 February 2007; accepted 14 February 2007
Available online 25 February 2007

Abstract

The surface of commercial $LiCoO_2$ was modified by molten salt method. The structure and electrochemical and thermal performances of the $MgCl_2$-treated $LiCoO_2$ were characterized by X-ray diffraction (XRD), scanning electron microscopy (SEM), differential scanning calorimetry (DSC), X-ray photoelectron spectroscopy and galvanostatic cycling. It is found that surface modification improves the structural and thermal stability as well as the rate performance of $LiCoO_2$. These improvements were attributed to the formation of homogeneous solid solution on the surface of the $LiCoO_2$ particle.

Keywords: Surface modification; Molten salt; Performance improvement; Lithium ion batteries

1. Introduction

$LiCoO_2$ is the most commercialized cathode material for lithium ion batteries because of its favorable features such as high energy density, low self-discharge rate and excellent cycle life. However, its available specific capacity remains only *ca.* 140 mAh g^{-1} in a practical battery, only roughly half of its theoretical capacity (274 mAh g^{-1}). Higher capacity can be obtained by charging the material to higher potentials (>4.2 V *versus* Li^+/Li). Nevertheless, this will lead to severe structural deterioration due to irreversible phase transitions [1] and obvious electrolyte decomposition because of the formation of strong oxidizing oxygen at deep delithiation states [2].

Elemental substitution has proved an effective method to improve the structural stability of the cathode materials. However, the improvement of the structural stability was realized at the expense of specific capacity [3–8].

Surface chemistry is of great importance to the performance of the electrode [9]. Recent studies show that coating the $LiCoO_2$ particles with oxides such as Al_2O_3 [10,11], MgO [12], ZrO_2 [13], TiO_2 [13], SnO_2 [14], CeO_2 [15], ZnO [16], P_2O_5 [17] and SiO_2 [18] helps to suppress capacity fading at deep charge states (>4.2 V). Many researchers try every effort to coat the $LiCoO_2$ surface as compactly as possible because it was believed that the coating layer helps to avoid the direct contact between the electrolyte and the active cathode material and, therefore, the reaction between them. Our previous studies [19,20], on the other hand, indicated that even compact coating cannot prevent the corrosion of $LiCoO_2$ by the acidic electrolyte. Surface coating increases the acidity of the electrolyte by forming Lewis acids via interaction with the electrolyte rather than scavenges the acidic species in the electrolyte. Previous studies also indicated that the solid solution formed near the surface of $LiCoO_2$ during electrochemical cycling for MgO-coated $LiCoO_2$ and during $LiAlO_2$-coating on $LiMn_2O_4$ [21] improved the structural stability of the cathode materials.

Molten salt method is one of the simplest means to prepare pure and stoichiometric multi-component oxide powders. The molten salts, characteristic of low melting point but high decomposition temperature, work as solvent or reacting species or sometimes both [22,23]. This method has found applications in synthesis of electrode materials [24–27] at rather low temperatures and in a short time because the diffusion of the ions is much quicker in the molten salt than in the solid. We believe that this method can also be used to modify the surface chemistry of $LiCoO_2$ by controlling the temperature, time and other

* Corresponding author. Tel.: +86 10 82649050; fax: +86 10 82649050.
E-mail address: wangzx@aphy.iphy.ac.cn (Z. Wang).

0378-7753/$ – see front matter © 2007 Elsevier B.V. All rights reserved.
doi:10.1016/j.jpowsour.2007.02.036

Table 1
Molar proportions of the chemicals in molten salt process

	$MgCl_2{\cdot}6H_2O$	$LiCoO_2$	$LiOH{\cdot}H_2O$
I	5	85	10
II	10	75	15
III	15	65	20
IV	20	55	25

conditions of the molten salt reaction. In this work, we improve the performances of commercial $LiCoO_2$ by bathing it in $MgCl_2$ molten salt to form a homogeneous modification layer.

2. Experimental

$MgCl_2{\cdot}6H_2O$ (99.0%, Beijing Shuanghuan Chemical Reagent Company), $LiOH{\cdot}H_2O$ (98.0%, Guangdong Longxi Chemicals) and commercial $LiCoO_2$ (Nippon Chemicals, battery grade; ~5 μm in diameter) were carefully mixed in a mortar at the required ratios (Table 1). $LiOH{\cdot}H_2O$ was used here to increase the Li content in the molten salt so as to compensate the lost lithium due to concentration difference in and out of the $LiCoO_2$ particles. The mixture was transferred to a muffler furnace when the temperature of the latter reached 750 °C. It was taken out after 2 h and cooled down outside the furnace to room temperature. The mixture was then washed with distilled water and filtered three times. Finally, the precipitates were heated at 100 °C for more than 12 h. Surface-modified $LiCoO_2$ was thus obtained. For comparison, the commercial $LiCoO_2$ was also annealed in the same way as the above samples.

X-ray diffraction (XRD) was carried out on a Holland X'Pert Pro MPD X-ray diffractometer equipped with a monochromatized Cu Kα radiation (λ = 1.5418 Å). The morphology of the samples was observed on a Hitachi S-4000 scanning electron microscope (SEM). Inductively coupled plasma (ICP) was conducted on ICP-8000 (Shimazu Co.) to determine the atomic ratio of the samples.

Descriptions of the electrode preparation and button-type test cell assembly can be found in Ref. [19]. The cells were charged and discharged on a LAND BT1-10 battery tester between 2.5 V *versus* Li^+/Li and various charge cut-off potentials. The ac impedance measurements were performed using an IM6e (Zahner Electric) impedance analyzer over a frequency range from 100 kHz to 5 mHz.

Differential scanning calorimetry (DSC) analysis was carried out on NETSCH STA 449 C in air by sealing the charged cathode sheet in an Al crucible in dry Ar and heated from 25 to 500 °C at a rate of 5 °C min^{-1}.

3. Results and discussion

Fig. 1 illustrates the morphologies of commercial and molten salt-treated $LiCoO_2$. It is seen that the surface of the 5% (not

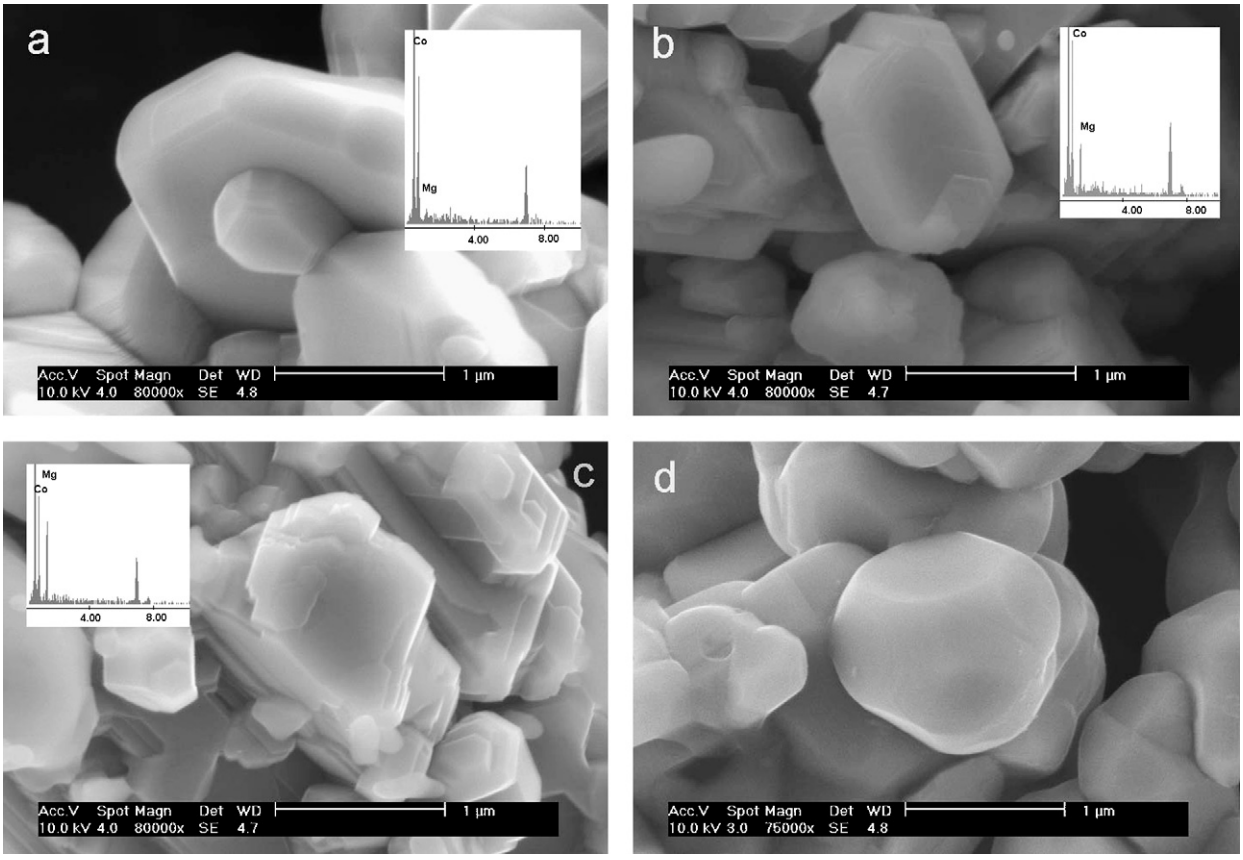

Fig. 1. Surface morphology of: (a) 10%, (b) 15%, (c) 20% $MgCl_2$ treated and (d) commercial $LiCoO_2$ (the insets are the corresponding EDAX patterns of the surface-modified $LiCoO_2$).

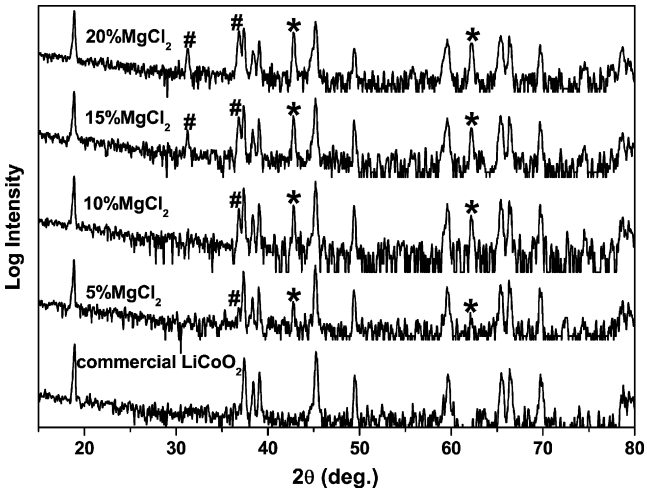

Fig. 2. Logarithm-scaled XRD patterns of $LiCoO_2$ before and after molten salt process at 750 °C for 2 h (*MgO, #Co_3O_4).

shown) and 10% $MgCl_2$-treated $LiCoO_2$ is very clean and smooth, without any radicals, very similar to that of commercial $LiCO_2$ annealed at 750 °C. However, the inset EDAX patterns demonstrate the existence of Mg on the $LiCoO_2$ surface. With increasing content of $MgCl_2$, the content of Mg increases and the $LiCoO_2$ surface becomes rough.

Fig. 2 shows the XRD patterns of $LiCoO_2$ before and after molten salt treatment. Besides hexagonal $LiCoO_2$, diffraction peaks of MgO and Co_3O_4 are observed after $MgCl_2$ processing. MgO is believed to be the reaction product between $MgCl_2$ and LiOH at high temperature while Co_3O_4 derives from $LiCoO_2$ when some lithium of the latter is lost. Calculation indicates that molten salt treatment does not lead to obvious changes in the lattice parameters of $LiCoO_2$. This is true even when the content of $MgCl_2$ increases to 20%. This means that the MgO and Co_3O_4 are formed at or near the surface of the $LiCoO_2$ particles but the hexagonal structure of bulk $LiCoO_2$ remains unchanged. More MgO and Co_3O_4 are detected when the content of $MgCl_2$ increases.

Table 2 shows the atomic ratios of Co, Li and Mg in the surface-modified $LiCoO_2$. It is clear that the loss of lithium ion is rather severe due to its content difference in and out of the $LiCoO_2$ particle. More lithium is lost when the $MgCl_2$ content increases.

It is known that formation of layered $LiMO_2$-type structure usually results from the size difference between the LiO_6 octahedra and the MO_6 octahedra. Therefore, the large cations preferentially occupy the lithium site if the layered $LiMO_2$ material is Li-deficient. As the radius of Mg^{2+} (0.072 nm) is very close to that of the Li^+ (0.076 nm), the Mg^{2+} ions tends to enter

Table 2
Atomic ratios of $LiCoO_2$ after molten salt processing

$MgCl_2$ content (%)	Co	Li	Mg
10	1	0.88	0.13
15	1	0.78	0.22
20	1	0.66	0.35

the interslab of $LiCoO_2$ to occupy the Li sites [28], resulting in the formation of Li–Mg–Co–O solid solution near the surface of $LiCoO_2$ particle. Clearly dissolution of Li^+ from $LiCoO_2$ in the molten salt accelerates the migration of Mg^{2+} into its interslab. Therefore, a thin layer of solid solution is formed at or near the surface of Li-deficient $LiCoO_2$, though Kweon et al. [29] and Kweon and Park [30] reported that only a small amount of Mg^{2+} can diffuse into the well-crystallized $Li_xNi_{1-y}Co_yO_2$ and $LiSr_{0.002}Ni_{0.9}Co_{0.1}O_2$ at 750 °C for 10 h. Because of the controlled reaction time, we believe that only a thin layer of solid solution $Li_{1-y}Mg_yCoO_2$ is formed near the surface of the $LiCoO_2$ particles. Therefore, no traces of solid solution are detected with XRD.

Surface-sensitive X-ray photoelectron spectroscopy (XPS) was employed to find out any differences in the electronic structure before and after molten salt treatment to commercial $LiCoO_2$. However, no obvious changes were observed in the binding energies of Co2p and O1s because the binding energies of Co2p in different cobalt oxides are similar to each other (ref. 780.2 eV in CoO, 779.9 eV in Co_2O_3 and 780.2 eV in Co_3O_4). Comparison of the integrated peaks indicates that the intensity ratio of Li1s *versus* Co3p decreases while the intensity ratio of Mg2p *versus* Co3p increases after molten salt treatment. This can be evidence for the formation of surface solid solution ($Li_{1-x}Mg_xCoO_2$) on $LiCoO_2$ (Fig. 3).

The formation of a surface solid solution is expected to improve the performance of $LiCoO_2$ material. Fig. 4a shows the charge/discharge profiles of the commercial and $MgCl_2$-treated $LiCoO_2$. The discharge plateau of commercial $LiCoO_2$ is rather steep in the first cycle but becomes flat in the subsequent cycles. The capacity retention of these two materials can be seen more clearly in Fig. 4b. The 750 °C annealed commercial $LiCoO_2$ has an initial discharge capacity of 131 mAh g^{-1}. Its capacity reaches 143 mAh g^{-1} after eight cycles. In the subsequent cycles, however, its capacity quickly degrades. It fades to 110 mAh g^{-1} after 60 cycles, corresponding to a capacity retention of 84%. In contrast, the discharge capacity of

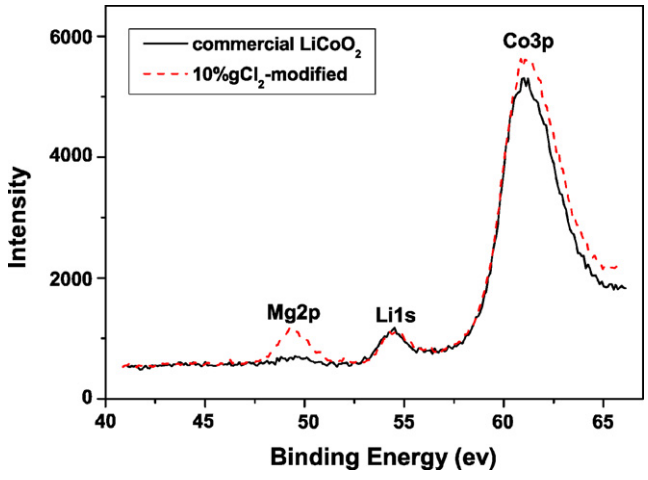

Fig. 3. Comparison of the X-ray photoelectron spectra of Li1s, Mg2p and Co3p on commercial $LiCoO_2$ simply annealed at 750 °C/2 h in air and bathed in molten $MgCl_2$ at 750 °C/2 h.

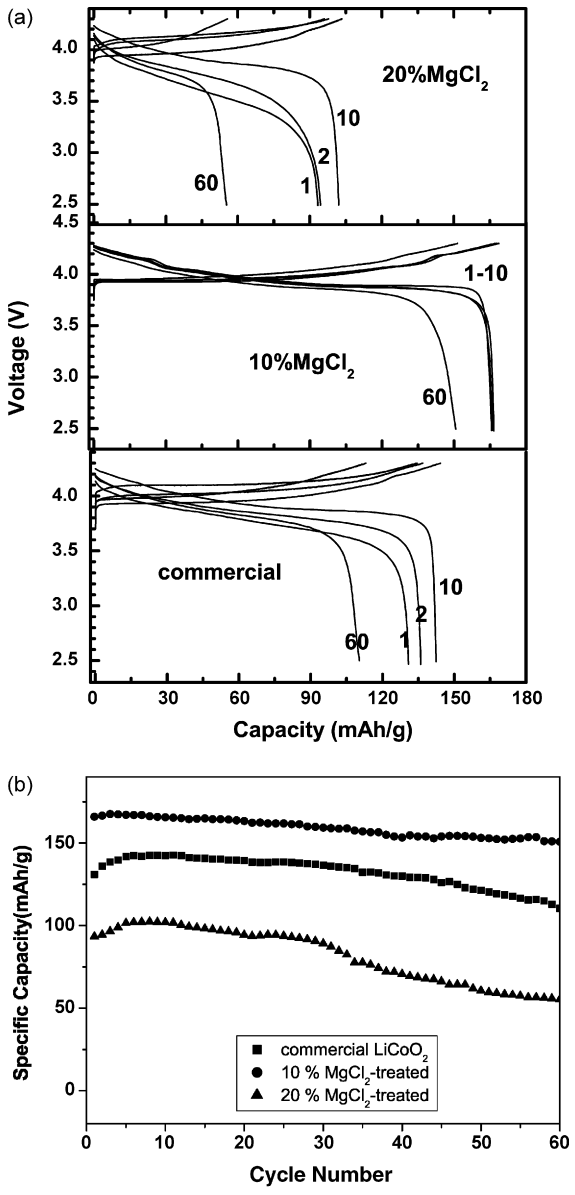

Fig. 4. Charge/discharge profiles: (a) and cycle number dependence of the discharge specific capacity and (b) of commercial $LiCoO_2$ annealed at 750 °C, 10 and 20% $MgCl_2$-processed $LiCoO_2$ cycled between 2.5 and 4.3 V at 0.2 mA.

the 10% $MgCl_2$-treated $LiCoO_2$ is high (166 mAh g^{-1}) in the initial cycling. In the subsequent cycles, this capacity further increases, reaching its maximum, 167 mAh g^{-1}, after six cycles. This value keeps fairly stable in the subsequent cycling processes. The capacity fades from 166 mAh g^{-1} in the 1st cycle to 151 mAh g^{-1} in the 60th cycle, corresponding to a capacity retention of 91%, indicating the improved structural reversibility of the surface-modified $LiCoO_2$ at deep delithiation states. However, excess addition of $MgCl_2$ (20%) decreases the capacity and deteriorates the reversibility of the material.

Usually the exothermic temperature becomes low when the cathode material is charged to a high voltage. This will lead to safety problems when the battery is overcharged or otherwise abused. Fig. 5 compares the DSC traces of commercial (before and after 750 °C/2 h annealing) and 10% $MgCl_2$-treated

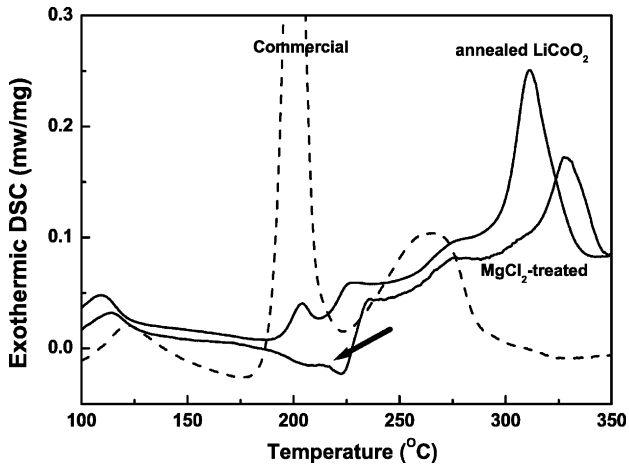

Fig. 5. DSC traces of commercial before (6.6 mg) and after (7.2 mg) 750 °C/2 h processed and 10% $MgCl_2$-treated $LiCoO_2$ (5.9 mg) charged to 4.7 V (the arrow is for the exothermic peak of 10% $MgCl_2$-modified $LiCoO_2$).

$LiCoO_2$ charged to 4.7 V. It is seen clearly that after 750 °C/2 h processing, the exothermic reaction temperature of $LiCoO_2$ charged to 4.7 V is delayed from 194 °C for the annealed commercial $LiCoO_2$ to 204 °C for the $MgCl_2$-treated $LiCoO_2$. In addition, the exothermic amount is sharply reduced. Therefore, 10% $MgCl_2$ treatment also improves the thermal stability of the material at charged state.

Indeed the rate performance and cycling performance of commercial $LiCoO_2$ can be enhanced by simple heat treatment because the insulating impurities such as Li_2CO_3 on $LiCoO_2$ is eliminated during this process, as Chen and Dahn [33] reported. However, the same authors also pointed out that heat treatment alone cannot improve the thermal stability of $LiCoO_2$. Fig. 6 compares the FTIR spectra of commercial $LiCoO_2$ before and after heat treatment at 750 °C for 2 h. The FTIR spectra of commercial $LiCoO_2$ and $LiCoO_2$ annealed in air at 750 °C for 2 h are almost the same to each other, indicating that surface species on long-term stored commercial $LiCoO_2$ is very low. The FTIR spectra of commercial MgO and Co_3O_4 are also presented for reference. Clearly MgO and Co_3O_4 are observed on the surface of the $MgCl_2$-molten salt processed $LiCoO_2$. That is, the FTIR spectrum of $LiCoO_2$ annealed in 10% $MgCl_2$ at 750 °C for 2 h can be regarded as a simple addition of the weighed spectra of $MgCl_2$, Co_3O_4 and $LiCoO_2$. No other species/phases are recognizable. Therefore, the improved structural stability (including the improved cycling performance and the thermal stability) should be attributed to the surface modification though we believe that the surface impurities on commercial $LiCoO_2$ can be removed during the molten salt treatment.

The above results show that molten salt processing is effective in improving the structural stability of $LiCoO_2$. This improvement is attributed to the pillaring effect of the Mg^{2+} ions in the interslab. Pouillerie et al. [28] believed that the existence of Mg^{2+} in $LiNiO_2$ hinders the collapse of the hexagonal structure at the end of the charge process. Analogously, oxidation of the Co^{3+} ions induces a local collapse of the interslab space in the $Li_{1-x}CoO_2$ system, making it difficult for the lithium ions to diffuse and re-intercalate. In the $Li_{1-x-y}Mg_yCoO_2$, however, the

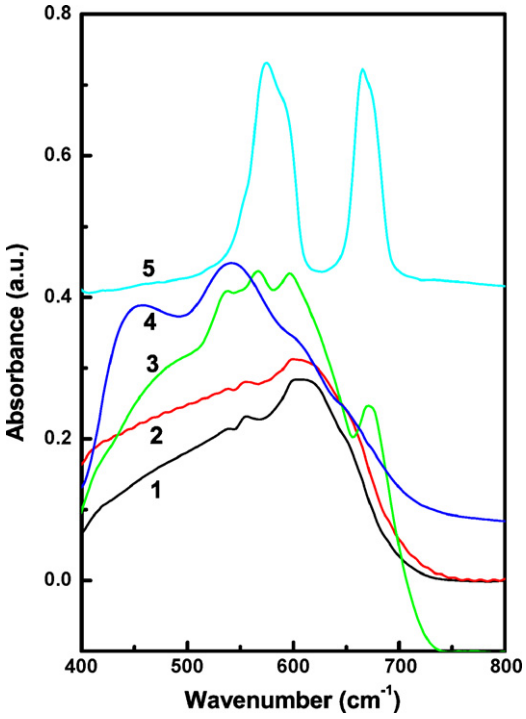

Fig. 6. Comparison of the FTIT spectra of commercial $LiCoO_2$ (1), $LiCoO_2$ annealed at 750 °C for 2 h in air (2), $LiCoO_2$ annealed in 10% $MgCl_2$ at 750 °C for 2 h (3), and commercial Co_3O_4 (4) and MgO (5).

electrochemically inactive Mg^{2+} ions work as pillars and suppress the collapse of the CoO_2 interslab. The Mg^{2+} ions in the interslab do not hinder the lithium diffusion because they have similar ionic size as the Li^+ ions. These Mg^{2+} ions have another effect. They suppress the dissolution of the highly oxidized Co^{4+} from the 2D lithium layer to the electrolyte because the Mg–O bonding is stronger than the Co–O bonding, thus alleviate the electrolyte decomposition due to attack of the oxidizing Co^{4+} ions.

Fig. 4 also demonstrates the remarkable polarization of commercial $LiCoO_2$. This polarization explains the low charge/discharge capacity of commercial $LiCoO_2$. However, as MgO is electron- and ion-insulating and electrochemically inactive, coating MgO on the surface of $LiCoO_2$ particle will increase its polarization. This is contradictive to the observed low polarization of surface-modified $LiCoO_2$. An explanation is that the Mg^{2+} ions migrate into the lattice of Li-deficient $LiCoO_2$ during cycling and the thickness of the solid solution near the surface of $LiCoO_2$ is increased. Tukamoto and West [31] reported that doping Mg^{2+} in $LiCoO_2$ creates more Co^{4+} ions and enhances the conductivity of $LiCoO_2$ as well as its structural stability. Meanwhile, Li^+ vacancies are generated to balance the excess covalence, greatly enhancing the conductivity of $LiCoO_2$ and resulting in the decrease of polarization of the system, beneficial for the Li^+ transportation [31].

Fig. 7 exhibits the rate performance of commercial and 10% $MgCl_2$-treated $LiCoO_2$ at 25 °C. The cells are charged galvanostatically to 4.5 V at a current of 0.1 mA but discharged to 2.5 V at different current densities. It is seen that the capacity of commercial $LiCoO_2$ decreases sharply with increasing current density.

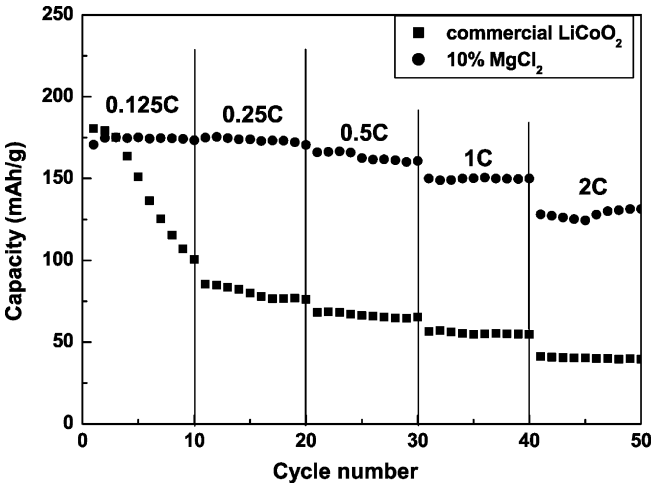

Fig. 7. Comparison of the rate performances of commercial and 10% $MgCl_2$-treated $LiCoO_2$ at different current densities ($1C = 190\ mAh\ g^{-1}$).

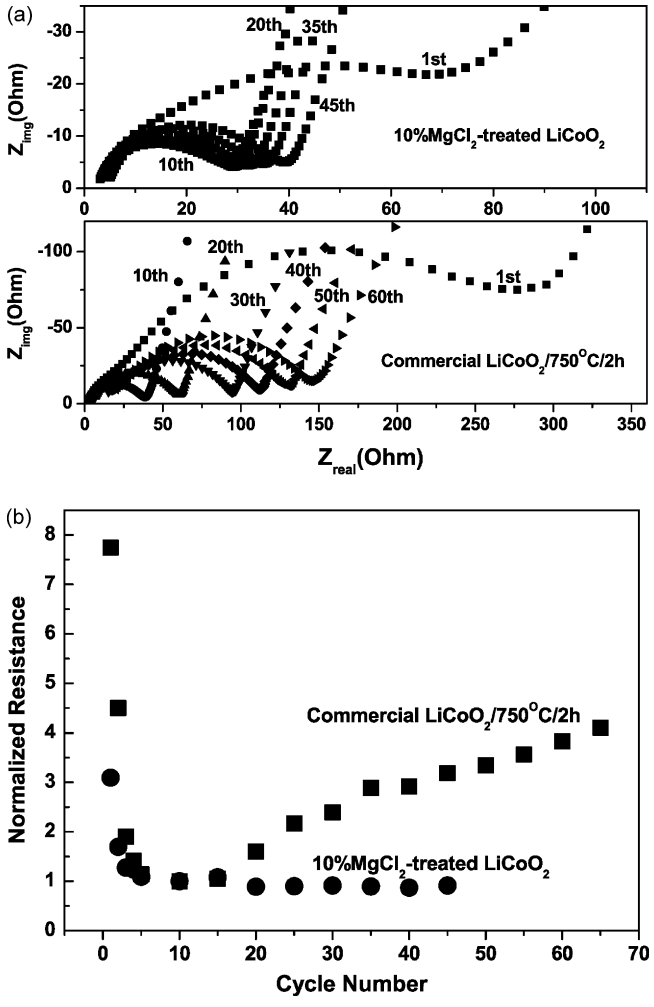

Fig. 8. Comparison of the dependence of: (a) Nyquist plots and (b) the normalized impedance of commercial and 10% $MgCl_2$-treated $LiCoO_2$ with cycling numbers (the unexpectedly large impedance of the first cycle of commercial $LiCoO_2$ electrode arises from fitting error because the semicircles of the first cycle is rather irregular).

On the contrary, the capacity decrease of the 10% $MgCl_2$-treated $LiCoO_2$ is much slower with increasing current density. The improvement of rate performance is attributed to the enhanced conductivity of the 10% $MgCl_2$-treated $LiCoO_2$.

In order to understand the improved rate performance of the surface-modified $LiCoO_2$, the Li/$LiCoO_2$ cell was aged for 2 days to reach equilibrium before the ac impedance spectra were recorded (Fig. 8a). The semicircle in the high-frequency region of the Nyquist plot is mainly the contribution of the solid electrolyte interphase (SEI) on the electrode [32]. It is seen that the impedance of the commercial $LiCoO_2$ electrode increases sharply with cycling while that of the 10% $MgCl_2$-treated $LiCoO_2$ increases very slowly.

As the commercial $LiCoO_2$ and the 10% $MgCl_2$-treated $LiCoO_2$ are different electrodes, their impedances cannot be quantitatively compared directly. Therefore, the impedance of each electrode after 10 cycles at discharge state is defined as 1 (normalized). The evolutions of the impedance of these two materials with cycling are compared in Fig. 8b. The impedance of commercial electrode increases monotonously with cycling while that of the 10% $MgCl_2$-treated $LiCoO_2$ increases very little. Chen and Dahn [33] pointed out that impedance growth was responsible for the rapid capacity fading of $LiCoO_2$ cycled to 4.5 V *versus* Li^+/Li. These facts partially explain the good capacity retention of 10% $MgCl_2$-treated $LiCoO_2$ (Fig. 4) and insure the excellent rate performance of the materials (Fig. 7). Enhanced structural stability is another reason for the improved reversibility of the surface-modified material.

4. Conclusions

The electrochemical and thermal performances of commercial $LiCoO_2$ are significantly improved by modifying its surface via molten-salt treatment. The migration of Mg^{2+} ions into the lattice of Li^+ deficient $LiCoO_2$ during molten salt processing and during electrochemical cycling takes important roles. The formation of surface solid solution stabilizes the structure of $LiCoO_2$, alleviates the reaction between oxidizing $Li_{1-x}CoO_2$ (charged $LiCoO_2$) and the electrolyte, suppresses the Co^{4+} dissolution at charged state and enhances the conductivity of, at least, the surface layer. The molten salt method is superior to the traditional coating method in surface modification because a solid solution can be formed during annealing and the coating layer is homogeneous.

Acknowledgements

This work was financially supported by the National 973 Program (No. 2002CB211800), the National Science Foundation (NSFC, No. 50272080) of China and Beijing Key Laboratory for Nano-Photonics and Nano-Structure.

References

[1] T. Ohzuku, A. Ueda, J. Electrochem. Soc. 141 (1994) 2972.
[2] Z.X. Wang, X.J. Huang, L.Q. Chen, J. Electrochem. Soc. 150 (2003) A199.
[3] S. Levasseur, M. Mĭenĭetrier, C. Delmas, J. Electrochem. Soc. 149 (2002) A1533.
[4] S. Levasseur, M. Mĭenĭetrier, C. Delmas, J. Power Sources 112 (2002) 419.
[5] S. Madhavi, G.V. Subba Rao, B.V.R. Chowdari, S.F.Y. Li, Electrochim. Acta 48 (2002) 219.
[6] S. Madhavi, G.V. Subba Rao, B.V.R. Chowdari, S.F.Y. Li, J. Electrochem. Soc. 148 (2001) A1279.
[7] G. Ceder, Y.M. Chiang, D.R. Sadoway, M.K. Aydinol, Y.I. Jang, B. Huang, Nature 392 (1998) 694.
[8] S.T. Myung, N. Kumagai, S. Komaba, H.T. Chung, Solid State Ionics 139 (2001) 47.
[9] D. Aurbach, K. Gamosky, B. Markovsky, G. Salitra, Y. Gofer, H. Heider, R. Oesten, M. Schmidt, J. Electrochem. Soc. 147 (2000) 1322.
[10] J. Cho, Y.J. Kim, B. Park, Chem. Mater. 12 (2000) 3788.
[11] Z.X. Wang, L.J. Liu, L.Q. Chen, X.J. Huang, Solid State Ionics 148 (2002) 335.
[12] Z.X. Wang, C. Wu, L.J. Liu, F. Wu, L.Q. Chen, X.J. Huang, J. Electrochem. Soc. 149 (2002) A466.
[13] J. Cho, Y.J. Kim, T.J. Kim, B. Park, Angew. Chem. Int. Ed. 40 (2001) 3367.
[14] J. Cho, C.S. Kim, S.I. Yoo, Electrochem. Solid-State Lett. 3 (2000) 362.
[15] H.W. Ha, K.H. Jeong, N.J. Yun, M.Z. Hong, K. Kim, Electrochim. Acta 50 (2005) 3764.
[16] T. Fang, J.G. Duh, S.R. Sheen, J. Electrochem. Soc. 152 (2005) A1701.
[17] J. Cho, J.G. Lee, B. Kim, B. Park, Chem. Mater. 15 (2003) 3190.
[18] H. Omanda, T. Brousse, C. Marhic, D.M. Schleich, J. Electrochem. Soc. 151 (2004) A922.
[19] Y. Bai, N. Liu, J.Y. Liu, Z.X. Wang, L.Q. Chen, Electrochem. Solid-State Lett. 9 (2006) A552.
[20] J.Y. Liu, N. Liu, D.T. Liu, Y. Bai, L.H. Shi, Z.X. Wang, L.Q. Chen, J. Electrochem. Soc. 154 (2007) A55.
[21] Y.C. Sun, Z.X. Wang, L.Q. Chen, X.J. Huang, J. Electrochem. Soc. 150 (2003) A1294.
[22] C.C. Chiu, C.C. Li, S.B. Desu, J. Am. Ceram. Soc. 74 (1991) 38.
[23] K.H. Yoon, Y.S. Cho, D.H. Lee, D.H. Kang, J. Am. Ceram. Soc. 76 (1991) 1373.
[24] W. Tang, H. Kanoh, K. Ooi, Electrochem. Solid-State Lett. 145–146 (1998) 1.
[25] X. Yang, W. Tang, H. Kanoha, K. Ooi, J. Mater. Chem. 9 (1999) 2683.
[26] C. Han, Y. Hong, C.M. Park, K. Kim, J. Power Sources 92 (2001) 95.
[27] H.Y. Liang, X.P. Qiu, S.C. Zhang, Z.Q. He, W.T. Zhu, L.Q. Chen, Electrochem. Commun. 6 (2004) 505.
[28] C. Pouillerie, L. Croguennec, Ph. Biensan, P. Willmann, C. Delmas, J. Electrochem. Soc. 147 (2000) 2061.
[29] H.J. Kweon, S.J. Kim, D.G. Park, J. Power Sources 88 (2000) 255.
[30] H.J. Kweon, D.G. Park, Electrochem. Solid-State Lett. 3 (2000) 128.
[31] H. Tukamoto, A.R. West, J. Electrochem. Soc. 144 (1997) 3164.
[32] S.S. Zhang, K. Xu, T.R. Jow, Electrochem. Solid-State Lett. 5 (2002) A92.
[33] Z. Chen, J.R. Dahn, Electrochim. Acta 49 (2004) 1079.